Thin Wire Representation of the Vertical Conductor in Surge Simulation

Md. Osman Goni, Eiji Kaneko, Hideomi Takahashi

Abstract— **Simulation of very fast surge phenomena in a three-dimensional (3-D) structure requires a method based on Maxwell's equations, such as the FDTD (finite difference time domain) method or the MoM (method of moments), because circuit-equation-based methods cannot handle the phenomena. This paper describes a method of thin wire representation of the vertical conductor system for the FDTD method which is suitable for the 3-D surge simulation. The thin wire representation is indispensable to simulate electromagnetic surges on wires or steel frames of which the radius is smaller than a discretized space step used in the FDTD simulation. A general surge analysis program named VSTL (Virtual Surge Test Lab.) based on the Maxwell equations formulated by the FDTD method is used to simulate the surge phenomena of a vertical conductor, including the effects of ground plane and without ground plane. By use of the Maxwell equations, VSTL is inherently able to take into account the three-dimensional geometrical features of a simulated structure unlike EMTP-type circuit-based transient programs. Comparisons between calculated results by the FDTD method, theoretical results and computed results by the NEC-2 (Numerical Electromagnetic Code) based on the MoM are presented to show the accuracy of the thin wire representation.**

Keywords— **FDTD method, Maxwell equations, thin wire, surge analysis, Numerical electromagnetic field analysis, vertical conductor.**

I. INTRODUCTION

CONVENTIONAL surge problems have successfully been solved by circuit theory, where transmission lines consisting of wires parallel to the earth surface are modeled by distributed-parameter circuit elements and the other components by lumped-parameter circuit elements [1]. The distributed-parameter circuit theory assumes plane-wave propagation that is a reasonable and accurate approximation for the transmission lines, and this assumption enables handling of the electromagnetic wave propagation within the circuit theory. On the other hand, very fast surge phenomena in a three-dimensional (3-D) structure, which includes surge propagation in a transmission tower and in a tall building, cannot be approximated by plane-wave propagation. Thus, those phenomena cannot be dealt with by circuit theory but need to be solved by Maxwell's equation as an electromagnetic field problem. Nowadays, the surge propagation in a transmission tower needs to be analyzed for economical insulation design. Furthermore, in a tall building, it is also important to assess the interference of lightning surges with information devices inside the building.

The processing speed and the memory capacity of computers have rapidly been progressing, and the FDTD (finite difference time domain) method that solves the Maxwell's equations by the method of difference becomes a practical choice in the field of antenna analysis [2], [3]. At present, even a personal computer can be used for FDTD analysis, and these circumstances caused the authors to analyze vertical conductor surge response based on the FDTD method.

This paper describes the surge analysis program named VSTL (Virtual Surge Test Lab.) based on the FDTD method. VSTL has been developed by Noda *et al.* from scratch at CRIEPI since late 1999. and continuous development is being carried out. VSTL is one of the registered programs of CRIEPI which are available to Japanese electric power utilities and to non-profitable research groups in the world. The FDTD method divides the space of interest into cubic cells and directly calculates the electric and magnetic fields of the cells by discretizing the Maxwell equations, where the derivatives with respect to time and space are replaced by a numerical difference. Updating the procedure at each time step gives the transient solution of electric and magnetic fields. By use of the FDTD method, the developed program VSTL is inherently able to take into account the geometrical features of a simulated structure, unlike EMTP-type circuit-based transient programs. Thus, the program is advantageous to solve both of the following problem types:

(i) surge propagation on a three-dimensional circuit (3-D skeleton structure);

(ii) surge propagation inside a three-dimensional imperfectly conducting medium such as earth soil.

The MoM (method of moments) also numerically solves the Maxwell Equations [4], and the NEC-2 (Numerical Electromagnetic Code)is a well-known program based on MoM [5]. Although MoM efficiently solves the type (i) problems, it cannot solve the type (ii) ones except very simple cases, because the handing of three-dimensional current distribution in a imperfectly conducting medium is complicated [6]. On the other hand, FDTD is inherently able to solve both problem types efficiently. One weak point of FDTD is the treatment of a thin wire. Thus, a field correction method to accurately treat the radius of the thin wire is proposed in [7] and implemented in VSTL. This paper proposes a method to accurately represent the thin wire for the single vertical conductor in the FDTD simulation ("thin wire" is defined as a conductive wire of which the radius is smaller than the size of a discretized cell). Then, surge simulation results using NEC-2 for the thin wire representation of a vertical conductor are also presented.

One of the authors derived the formula of surge impedance with a ground plane: $Z = 60\{ln(2\sqrt{2}h/r_0) - 1.983\}\,(\Omega)$ and without a ground plane: $Z = 60\{ln(2\sqrt{2}h/r_0) - 1.540\}\,(\Omega)$ [8]. The theoretical formula of surge impedance with the ground plane is very close to the well known experimental formula of Hara *et al.* [9]. The theoretical values of surge impedance at $t = 2h/c$ agree satisfactorily with the experimental and computed results using NEC-2 [10], [11]. Finally, this paper shows the comparisons between the theoretical results and simulation results of surge impedance with ground plane and without ground plane, based on the FDTD method and NEC-2.

II. ALGORITHM

In the analysis of VSTL, the analysis space is defined as a rectangular-parallelepiped space. Arbitrary number of thin wire conductors, rectangular-parallelepiped conductors, and localized voltage and current sources are arbitrarily placed in the analysis space, and transient electric and magnetic fields are calculated. The bottom of the analysis space can be defined as an imperfectly-conducting medium such as earth, and each boundary of the analysis space can independently be defined as a perfectly-conducting plane or an absorbing plane. The waveform of a localized voltage or current at an arbitrary position is outputted as specified.

A. *FDTD Formulation*

There exist several different formulations of FDTD method. In order to precisely describe the proposed method of thin wire representation, the formulation used in this paper is briefly reviewed here. Assuming neither anisotropic nor dispersive medium in the space of interest, the Maxwell equations in Cartesian coordinates are

$$\nabla \times \boldsymbol{E} = -\mu \frac{\partial \boldsymbol{H}}{\partial t}, \quad \nabla \times \boldsymbol{H} = \epsilon \frac{\partial \boldsymbol{E}}{\partial t} + \sigma \boldsymbol{E}, \tag{1}$$

$$\nabla \cdot \boldsymbol{E} = \frac{\rho}{\epsilon}, \quad \text{and} \quad \nabla \cdot \boldsymbol{H} = 0. \tag{2}$$

where

- $\boldsymbol{E}$ electric field;
- $\boldsymbol{H}$ magnetic field;
- ρ charge density;
- ϵ permittivity;
- μ permeability;
- σ conductivity.

Discretizing the analysis space by a small length Δs in all the directions, the space is filled with cubes of which the sides are Δs, and each cube is called a *cell*. Assume that the number of divisions of the analysis space along the x coordinate is N_x, along the y coordinate N_y, and along the z coordinate N_z. The analysis space is given by the following range,

$$x = i\Delta s, (0 \le i \le N_x), \quad y = j\Delta s, (0 \le j \le N_y), \\ z = k\Delta s, (0 \le k \le N_z). \tag{3}$$

Equation (1) includes derivatives with respect to position x, y, z, and time t. In the FDTD formulation, representing values of electric and magnetic fields in a cell is shown in Fig. 1, and this yields the replacement of the derivatives with respect to x, y, and z in (1) with the following central difference,

$$\frac{\partial f(x)}{\partial x} \cong \frac{f(x + \Delta x/2) - f(x - \Delta x/2)}{\Delta s}. \tag{4}$$

In the above equation, f is a component of $\boldsymbol{E}$ or $\boldsymbol{H}$, and the same equation is valid also for y and z. The same central difference shown in the following equation replaces the derivatives with respect to time in (1), assuming that electric fields are calculated at time steps $t = n\Delta t\,(n = 0, 1, \cdots)$ and magnetic fields at $t = (n + 1/2)\Delta t\,(n = 0, 1, \cdots)$ by turns,

$$\frac{\partial f(t)}{\partial t} \cong \frac{f(t + \Delta t/2) - f(t - \Delta t/2)}{\Delta t}. \tag{5}$$

Applying (4) and (5) to (1) yields the following difference equations (e.g. ${E^n}_x(i + 1/2, j, k)$ represents x component electric field at position $x = (i + 1/2)\Delta s$, $y = j\Delta s$, $z = k\Delta s$, and at time $t = n\Delta t$, and the other components are expressed in the same manner),

$$\begin{aligned} E_x^n(i+\tfrac{1}{2},j,k) &= K_1 E_x^{n-1}(i+\tfrac{1}{2},j,k) \\ &+K_2\{H_z^{n-1/2}(i+\tfrac{1}{2},j+\tfrac{1}{2},k) - H_z^{n-1/2}(i+\tfrac{1}{2},j-\tfrac{1}{2},k) \\ &-H_y^{n-1/2}(i+\tfrac{1}{2},j,k+\tfrac{1}{2}) + H_y^{n-1/2}(i+\tfrac{1}{2},j,k-\tfrac{1}{2})\} \end{aligned} \tag{6}$$

$$\begin{aligned} E_y^n(i,j+\tfrac{1}{2},k) &= K_1 E_y^{n-1}(i,j+\tfrac{1}{2},k) \\ &+K_2\{H_x^{n-1/2}(i,j+\tfrac{1}{2},k+\tfrac{1}{2}) - H_x^{n-1/2}(i,j+\tfrac{1}{2},k-\tfrac{1}{2}) \\ &-H_z^{n-1/2}(i+\tfrac{1}{2},j+\tfrac{1}{2},k) + H_z^{n-1/2}(i-\tfrac{1}{2},j+\tfrac{1}{2},k)\} \end{aligned} \tag{7}$$

$$\begin{aligned} E_z^n(i,j,k+\tfrac{1}{2}) &= K_1 E_z^{n-1}(i,j,k+\tfrac{1}{2}) \\ &+K_2\{H_y^{n-1/2}(i+\tfrac{1}{2},j,k+\tfrac{1}{2}) - H_y^{n-1/2}(i-\tfrac{1}{2},j,k+\tfrac{1}{2}) \\ &-H_x^{n-1/2}(i,j+\tfrac{1}{2},k+\tfrac{1}{2}) + H_x^{n-1/2}(i,j-\tfrac{1}{2},k+\tfrac{1}{2})\} \end{aligned} \tag{8}$$

$$\begin{aligned} H_x^{n+1/2}(i,j+\tfrac{1}{2},k+\tfrac{1}{2}) &= H_x^{n-1/2}(i,j+\tfrac{1}{2},k+\tfrac{1}{2}) \\ &+K_3\{-E_z^n(i,j+1,k+\tfrac{1}{2}) + E_z^n(i,j,k+\tfrac{1}{2}) \\ &+E_y^n(i,j+\tfrac{1}{2},k+1) - E_y^n(i,j+\tfrac{1}{2},k)\} \end{aligned} \tag{9}$$

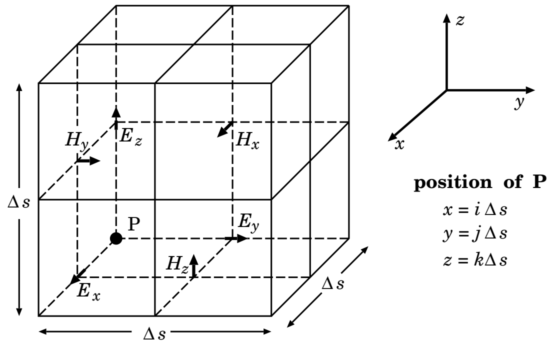

Fig. 1. Configuration of electric and magnetic fields in cell.

$$H_y^{n+1/2}(i+\frac{1}{2},j,k+\frac{1}{2}) = H_y^{n-1/2}(i+\frac{1}{2},j,k+\frac{1}{2}) + K_3\{-E_x^n(i+\frac{1}{2},j,k+1) + E_x^n(i+\frac{1}{2},j,k) + E_z^n(i+1,j,k+\frac{1}{2}) - E_z^n(i,j,k+\frac{1}{2})\} \quad (10)$$

$$H_z^{n+1/2}(i+\frac{1}{2},j+\frac{1}{2},k) = H_z^{n-1/2}(i+\frac{1}{2},j+\frac{1}{2},k) + K_3\{-E_y^n(i+1,j+\frac{1}{2},k) + E_y^n(i,j+\frac{1}{2},k) + E_x^n(i+\frac{1}{2},j+1,k) - E_x^n(i+\frac{1}{2},j,k)\}. \quad (11)$$

In the derivation of the above equations, an approximation $\sigma \boldsymbol{E}^{n-1/2} \cong \sigma\{\boldsymbol{E}^{n-1} + \boldsymbol{E}^n\}/2$ is used, and coefficients K_1, K_2, and K_3 are given by the following equations,

$$K_1 = \frac{1-\frac{\sigma\Delta t}{2\epsilon}}{1+\frac{\sigma\Delta t}{2\epsilon}}, \quad K_2 = \frac{\Delta t}{\epsilon\Delta s}\frac{1}{1+\frac{\sigma\Delta t}{2\epsilon}}, \quad K_3 = \frac{\Delta t}{\mu\Delta s}. \quad (12)$$

Equations (6)–(11) are the FDTD formulas of the Maxwell equations, and transient fields are obtained by calculating electric and magnetic fields alternately at time intervals $\Delta t/2$. Although (2) is not explicitly formulated, it is proven that (6)–(11) automatically satisfies (2) [2]. The general surge analysis program VSTL uses this FDTD formulation.

B. *Time Step and Space Step*

Equations (6)–(11) are considered as numerical integration, and stable integration is performed if the following condition is satisfied (Courant's condition) [2],

$$\frac{\Delta t}{\sqrt{\mu\epsilon}} \le \frac{\Delta s}{\sqrt{3}}. \quad (13)$$

On the other hand, the grid dispersion error is minimize when the above equation is an equality. Thus, the following formula is used in all calculations in this paper to determine time step Δt by user defined space step Δs:

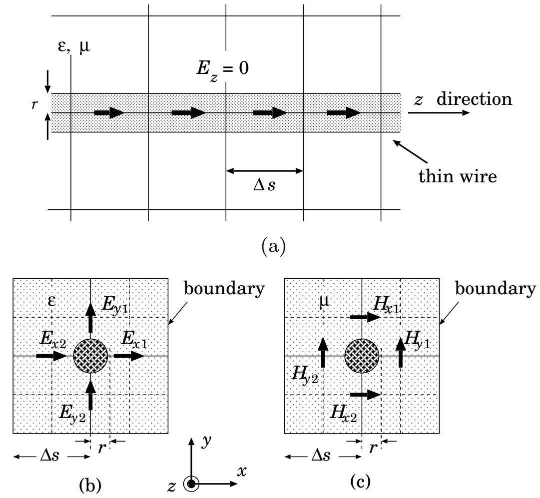

Fig. 2. Thin wire and configuration of adjacent electric and magnetic fields.

$$\Delta t = \Delta s\sqrt{\frac{\mu\epsilon}{3}}(1-\alpha). \quad (14)$$

α is a small positive value specified by the user in order to prevent instability of the numerical integration due to round-off error in (6)–(11).

III. THIN WIRE REPRESENTATION

If the space step were chosen to be small enough to represent the shape of wire's cross section, an accurate representation would be possible. However, it requires impractical computational resources at this moment. The thin wire is defined as a conductive wire of which the radius is smaller than the size of a cell in the FDTD simulation. In antenna simulations, the thin wire is mainly used to represent an antenna element–the most important part. In surge simulations, it is also important to represent wires (phase and ground wires of a transmission/distribution line) and steel frames of a building along which surges propagate. Umashankar et al. proposed a method of thin wire representation by correcting the adjacent magnetic fields of the wire according to its radius [12], and [13] reports that the method is valid for the calculation of radiated fields by an antenna. However, the Umashankar method cannot give accurate surge impedance [14].

A. *Modification of Permittivity and Permeability*

The FDTD method of thin wire representation corrects both the adjacent electric and magnetic fields of the wire according to its radius and gives accurate surge impedance. The correction of the fields is carried out by equivalently modifying the permittivity and permeability of the adjacent cells. Fig. 2(a) shows a wire with ra-

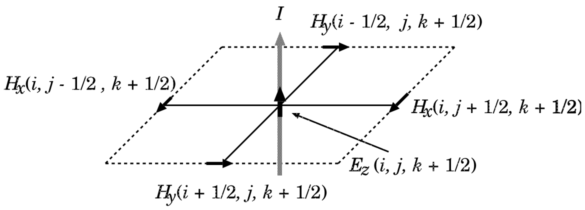

Fig. 3. Calculation of current by Ampere's Law.

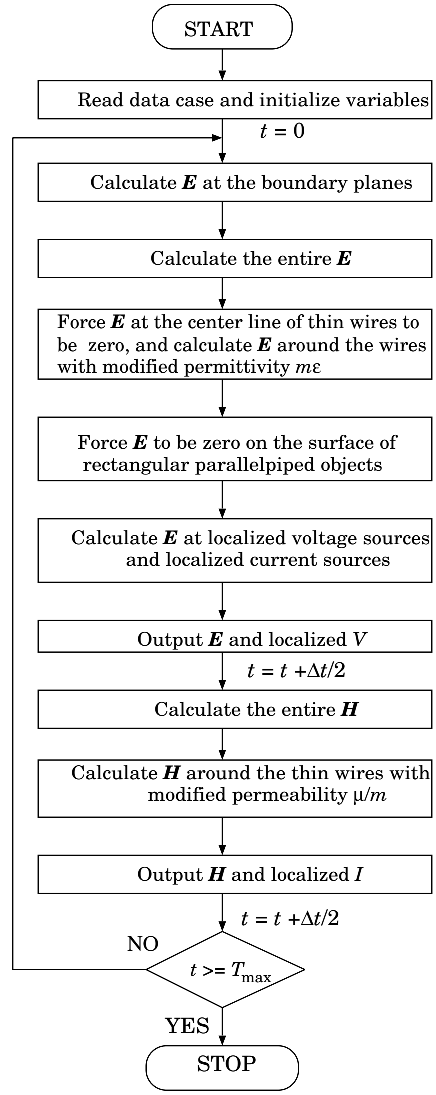

Fig. 4. Calculation procedure of VSTL.

dius r placed in the z direction, and the permittivity and permeability of the space are ϵ and μ. Fig. 2(b) shows the cross section of the wire with the adjacent electric fields, and Fig. 2(c) with the adjacent magnetic fields. In the FDTD method, a wire is, in principle, represented by forcing the electric fields along the center line of the wire to be zero, and E_z components are forced to be zero in this case. In order to take into account the effect of the thin wire radius r, the VSTL uses the following corrected permittivity to calculate the adjacent electric fields $E_{x1}, E_{x2}, E_{y1}, E_{y2}$ in (6)–(8),

$$\epsilon' = m\epsilon,$$

and the following corrected permeability to calculate the adjacent magnetic fields $H_{x1}, H_{x2}, H_{y1}, H_{y2}$ in (9)–(11),

$$\mu' = \mu/m,$$

where the correction factor m is given by

$$m = \frac{1.471}{\ln(\Delta s/r)}. \tag{15}$$

IV. GENERAL SURGE ANALYSIS PROGRAM

The general surge analysis program, named Virtual Surge Test Lab. (VSTL), which is based on the FDTD method and the proposed thin wire representation for the vertical conductor is briefly described in this section.

A. *Treatment of Boundaries*

Each boundary of the space of interest can independently be defined as a perfectly conducting plane or an absorbing plane. The perfectly conducting plane can easily be represented by forcing the tangential components of electric fields at the boundary to be zero. The second-order Liao's method is used to represent the absorbing plane, because it is more accurate and required less memory compared with other methods [15]. An open space can be assumed by applying the absorbing plane to all the boundaries of the space of interest.

B. *Imperfectly Conducting Earth*

The goal of the surge analysis is usually to find the solution of surge propagation in a 3-D skeleton structure above either an imperfectly or perfectly conducting earth. In the FDTD calculation, the representation of the conducting earth with resistivity ρ_e can be achieved by simply setting the value of σ in (12) to $1/\rho_e$ in the region defined as the copper plane.

C. *Rectangular-Parallelepiped Conductors*

The geometrical shape of most power equipment can be represented by a combination of several rectangular-parallelepiped objects. The rectangular-parallelepiped conductor is simply modeled by forcing the tangential electric fields on its surface to be zero.

D. *Localized Voltage and Current Sources*

Unlike the static electric fields, the transient electric fields do not satisfy $\nabla \times \boldsymbol{E} = 0$. Thus, in the analysis of transient fields, the voltage or the voltage difference does not make sense in general. But if we take notice of an electric field component of a cell, the voltage difference across a side of the cell can reasonably be defined as $V = E\Delta s$, because waves of which the wavelength is shorter than $\lambda = 2\Delta s$ do not propagate in the FDTD calculation due to the bandwidth limitation of Δs. Therefore, we can model a localized voltage source by forcing an electric field component at a specified position in a specified direction to be a specified waveform. For example, in order to place a voltage source of which the waveform is given by $V^n = V(n\Delta t)$ at $x = i\Delta s$, $y = j\Delta s$, $z = (k+1/2)\Delta s$ in the z direction, the following equation is used to force the electric field value,

$$E_z^n(i,j,k+1/2) = -\{V^n - RI^{n-1/2}\}/\Delta s, \qquad (16)$$

where R is the internal resistance of the voltage source specified by a user (it can be set to zero), and current I is given by the following equation as shown in Fig. 3,

$$\begin{aligned} I^{n-1/2} = \{&H_x^{n-1/2}(i, j-\tfrac{1}{2}, k+\tfrac{1}{2}) \\ &-H_x^{n-1/2}(i, j+\tfrac{1}{2}, k+\tfrac{1}{2}) \\ &+H_y^{n-1/2}(i+\tfrac{1}{2}, j, k+\tfrac{1}{2}) \\ &-H_y^{n-1/2}(i-\tfrac{1}{2}, j, k+\tfrac{1}{2})\}\Delta s. \end{aligned} \qquad (17)$$

In the case of a current source, because current itself is a general quantity even in the transient fields, it can be modeled by modifying an electric field component at a specified position in a specified direction as in the following example. In order to place a current source of which the waveform is given by $I^n = I(n\Delta t)$ at $x = i\Delta s$, $y = j\Delta s$, $z = (k + 1/2)\Delta s$ in the z direction, the following term is added to (8),

$$-\frac{\Delta t/\epsilon}{1+\frac{\sigma\Delta t}{2\epsilon}}\frac{I^{n-1/2}}{\Delta s^2}, \qquad \sigma = 1/(R\Delta s), \qquad (18)$$

and R is the internal resistance of the current source specified by a user.

E. *Calculation Procedure and Output*

The flow chart of the calculation procedure of VSTL is shown in Fig. 4. The output of VSTL includes the waveform of localized voltage differences and current intensities at a specified position in a specified direction. The waveform of the localized voltage difference is calculated by $V = E\Delta s$, and that of the current intensity by (17).

V. SIMULATION RESULTS OF VERTICAL CONDUCTOR

A. *With Ground Plane*

The modeling of a vertical conductor system is quite important as a basis of transmission tower modeling. A tower is approximated as a vertical cylinder having a height equal to that of the tower and a radius equal to the mean equivalent radius of the tower [16]. Fig. 5 shows a reduced-scale model of the vertical conductor system with a single cylindrical conductor of radius 5 mm. The vertical conductor is excited by a pulse generator (PG) via a current lead wire, and the tower-top voltage is defined as the voltage between the tower top and a voltage measuring wire. In the simulation with FDTD, the dimensions of the analysis space were $3.5\,\text{m}\times 2.5\,\text{m}\times 1.0\,\text{m}$ with space step $\Delta s = 2\,\text{cm}$. The time step was determined by (14) with $\alpha = 0.01$, and all the six boundaries of the cell were treated as second-order Liao's absorbing boundary. The thickness and the resistivity of the earth were set to 6 cm and $1.69\times10^{-8}\,\Omega$m. The PG was mod-

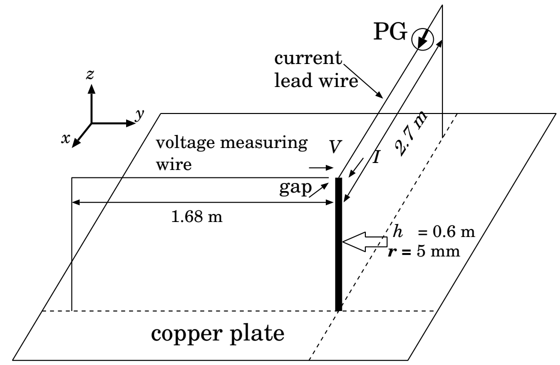

Fig. 5. Arrangement of the vertical conductor system (with ground plane).

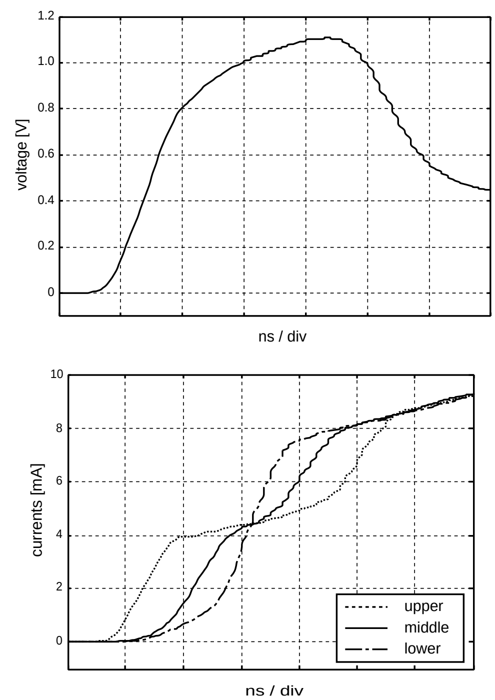

Fig. 6. Calculated waveforms of the voltage and currents (with ground plane).

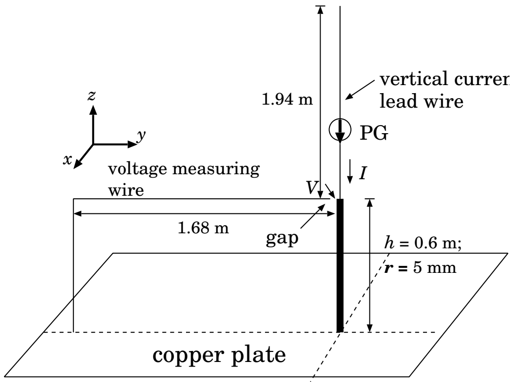

Fig. 7. Arrangement of the vertical conductor system (without ground plane).

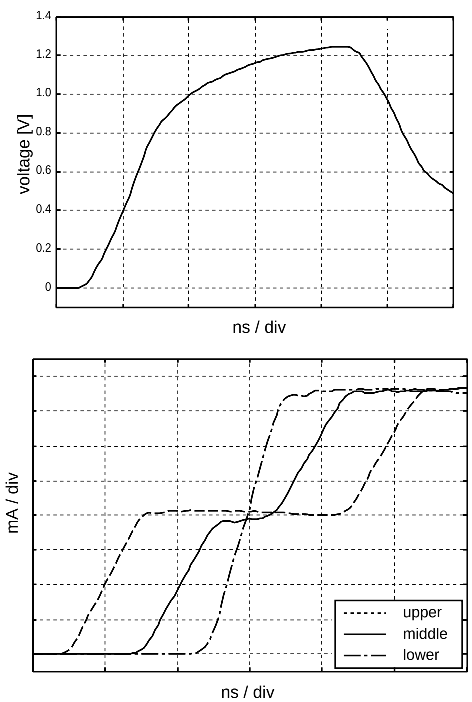

Fig. 8. Arrangement of the vertical conductor system (without ground plane).

eled by a current source, with internal resistance 0.5 kΩ. Fig. 6 shows the calculated results of voltage waveforms at the top of the vertical conductor and that of current waveforms in the different parts of it. The influence of the ground plane can be observed by realizing a small current which is induced in the vertical conductor before the actual surge current flows through it. This small magnitude of current is due to the fact that the electric field produced by the current injected in the horizontal current lead wire induces this current at the vertical conductor. The reflection phenomena of the current wave from the ground can be understood with these results.

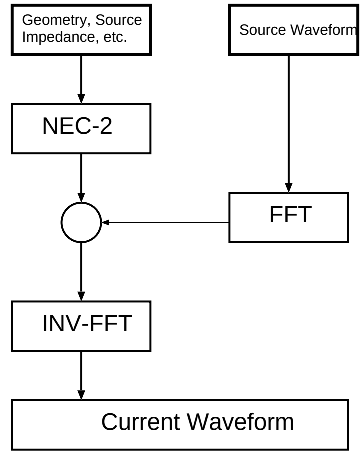

Fig. 9. Flow of the solution using NEC-2.

B. *Without Ground Plane*

A reduced-scale model of the vertical conductor system without ground plane is shown in Fig. 7. It is also the case of the lightning phenomena caused by the return stroke [17]. The pulse generator, in this case, is placed at the top of the vertical conductor and the current lead wire is extended vertically without connecting to the ground. The dimensions of the analysis space were $1.0\,\mathrm{m} \times 2.5\,\mathrm{m} \times 3.0\,\mathrm{m}$. All other parameters are the same as the case with the ground plane. Fig. 8 shows the waveform of conductor-top voltage and currents splitting into the vertical conductor.

C. *Computation Time*

It may be believed that the FDTD method is a time-consuming method. However, the progress of computers in terms of speed and memory is considerable, and even a personal computer can be used for FDTD calculations. In fact, the simulations presented in this paper were performed by a personal computer with Intel Celeron 700 MHz CPU and 192 MB RAM. Although the computation time absolutely depends on the cell size and the dimension of the analysis space, in this paper, the cell size is considered a lower value satisfying the Courant condition in order to obtain more accurate results of the surge response. Therefore, the computation time for the vertical conductor with ground plane is around 16 minutes and without ground plane is around 12 minutes.

VI. SURGE SIMULATION BY NEC-2

In this section, the NEC-2 (Numerical Electromagnetic Code) is employed for the analysis of surge response of the vertical conductor. It is a widely used three-dimensional electromagnetic modeling code based on the MoM (method of moments) [4] in the frequency domain, and is particularly effective in analyzing the electromagnetic response of antennas or other metallic structures

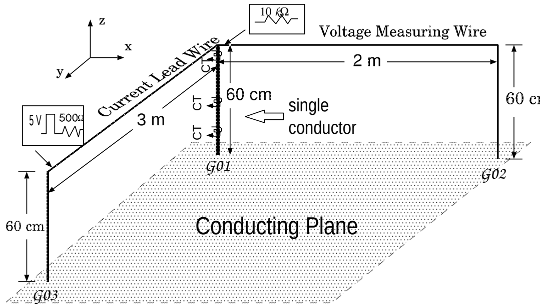

Fig. 10. Arrangement of the vertical conductor system (with ground plane).

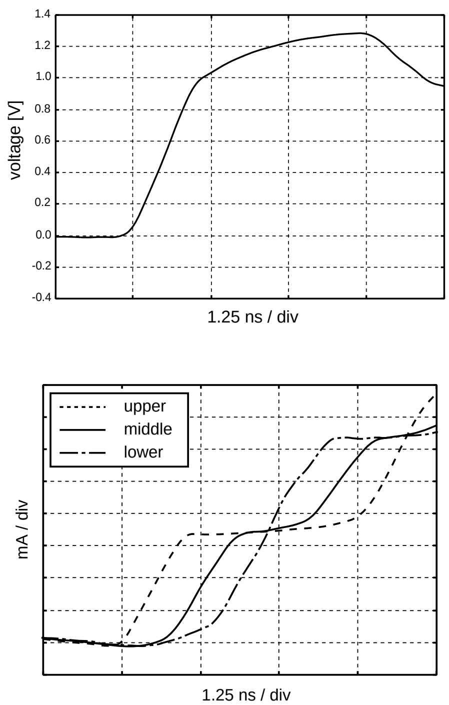

Fig. 11. Computed waveforms of voltage at the top and currents in the various parts of the vertical conductor in case with ground surface.

composed of thin wires. A vertical conductor system needs to be decomposed into thin wire elements, and the position, orientation and the radius of each element constitute the input data, along with the description of the source and frequencies to be analyzed. In the analysis, all the elements in the system are treated as perfect conductors. To solve the time-varying electromagnetic response, Fourier transform and inverse Fourier transform are used. The MoM requires that the entire structure be divided into wire segments that must be small compared to the wavelength. Once the model is defined, an excitation is imposed as a voltage source or a plane wave on one of the wire segments. The MoM approach is to determine the current on every segment due to the source and all the other currents by numerically solving the electric field integral equation. Fig. 9 shows the flow chart of the solution by NEC-2.

Fig. 10 shows the reduced-scale model of the vertical conductor system for the surge analysis using NEC-2. The arrangement of the current lead wire connected to the top of the vertical conductor with the existence of the ground plane is indicated in Fig. 10. The dimensions of the vertical conductor model are maintained the same as with the FDTD method in the previous section. A step current pulse generator having pulse voltage of 5 V in magnitude, rise-time of 1 ns and pulse width of 40 ns is used, which is meant to incorporate the influence of the induction from the lightning channel hitting the vertical conductor.

For the numerical analysis, the conductors of the system are divided into 5 cm segments. This segmentation must satisfy electrical consideration relative to the wavelength as: $0.001\lambda < \Delta L < 0.1\lambda$, where ΔL and λ are the segment length and wavelength respectively. The internal impedance of the pulse generator is 0.5 kΩ. The system of structures under analysis was postulated to be on perfectly conducting ground. Then we calculate the surge impedance, which is defined by the ratio of the instantaneous values of the voltage to the current at the moment of voltage peak.

A. With Ground Plane

Fig. 11 shows the simulation results by NEC-2. The influence of the reflected wave from the ground reaches the top of the conductor is observed at $t = 2h/c = 4$ ns exactly, which means that the travelling wave is propagating at the velocity of light. The computed waveforms of currents which are flowing through the vertical conductor are indicated by the mark 'CT' in Fig. 10. As the pulse generator is placed 300 cm from the vertical conductor, the current through the vertical conductor is delayed approximately 10 ns. The existence of the ground plane can also be observed in these current waveforms, where the field produced by the current injected horizontally induces currents of small magnitude before the actual surge current flows through the vertical conductor. These simulation results of currents and voltage waveforms in Fig. 11 obtained by NEC-2 are almost identical to the simulation results with the FDTD method in Fig. 6.

B. Without Ground Plane

A reduced-scale model of the vertical conductor system without a ground plane is indicated in Fig. 12. Here, the current lead wire is extended vertically to the top of the vertical conductor. The same PG is now used at the top without connecting to the ground. In both cases, the voltage measuring wire is stretched horizontally and connected to the ground. This termination condition does not affect the electromagnetic phenomena at the vertical conductor within 17.33 ns. All other parameters are maintained the same as the ground plane

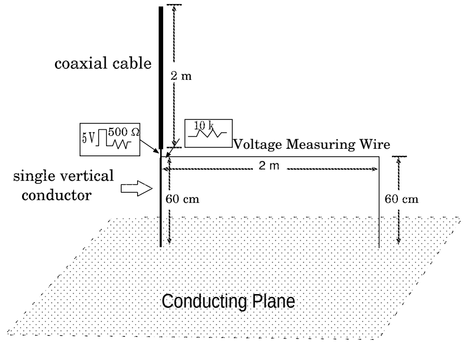

Fig. 12. Arrangement of the vertical conductor system (without ground plane).

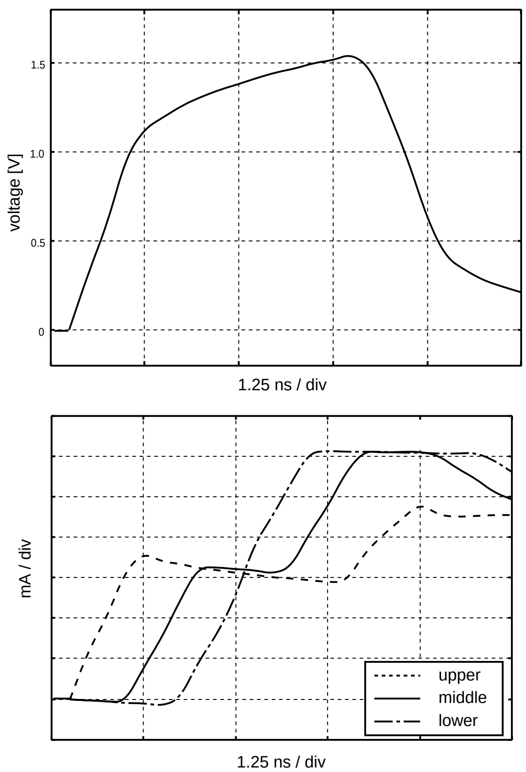

Fig. 13. Computed waveforms of voltage at the top and currents in the various parts of the vertical conductor in case with no ground surface.

case. The simulation results of voltage at the top of the vertical conductor and currents through different parts of it are shown in Fig. 13. However, in this analysis, the waveforms of current through the vertical conductor are somewhat different from the current waveforms of Fig. 11 at the starting region because of absence of the ground surface. Also, the current starts flowing instantly through the vertical conductor without being delayed.

C. *Computation Time*

Computation is carried out in the frequency range of 7.813 MHz to 4 GHz with an increment step of 7.813 MHz. This corresponds to the time range of 0 to 128 ns with 0.25 ns increments. The computation time for the output of NEC-2 block of the flow chart of Fig. 10, with a Intel Celeron 700 MHz processor with 192 MB RAM is about 56 seconds for the ground plane case and 30 seconds without ground plane case.

VII. THEORETICAL FORMULA OF SURGE IMPEDANCES

One of the author's theory is able to apply widely in case of ground surface and without ground surface. Suppose that a surge electric current is injected on the vertical conductor whose height is h and radius is r_0. Then the surge current wave is reflected at the ground of the perfect conductor and returns to the top of the vertical conductor.

Introducing the electric current reflectivity $\beta = 1$ and the magnetic field reflectivity $\gamma(\gamma_i, \gamma_r) = 0$, the theoretical formula of surge impedance which is very close to the well known experimental formula [9] is obtained as follows;

$$Z = 60(\ln(\frac{h}{2r_0}) - \frac{1}{4})$$

$$= 60(\ln(\frac{2\sqrt{2}h}{r_0}) - 1.983). \tag{19}$$

Equation (19) gives the surge impedance of the vertical conductor just after the occurrence of the reflection of the travelling wave propagating down from the top of the structure. However, if it is considered that $\beta = \gamma_i = \gamma_r = 1$, it became

$$V(t) = \frac{c\mu_0 I_0}{2\pi}\left(\ln\frac{(ct+2r_0)}{2r_0} - \frac{ct}{2(ct+r_0)}\right).$$

The above equation can be modified by substituting $ct = 2h$, where c is the velocity of light and assuming $h \gg r_0$ as follows;

$$Z = 60(\ln(\frac{h}{r_0}) - \frac{1}{2})$$

$$= 60(\ln(\frac{2\sqrt{2}h}{r_0}) - 1.540). \tag{20}$$

On the other hand, if there is no ground, the following formula is used [18],

$$V(t) = \int_0^{ct}(-E_i \cdot dl)$$

$$= \frac{c\mu_0 I_0}{2\pi}\left(\ln\frac{(ct+2r_0)}{2r_0} - \frac{ct}{2(ct+r_0)}\right).$$

Substituting $ct = 2h$ and assuming $h \gg r_0$ in the above equation, we get

$$Z = 60(\ln(\frac{h}{r_0}) - \frac{1}{2})$$

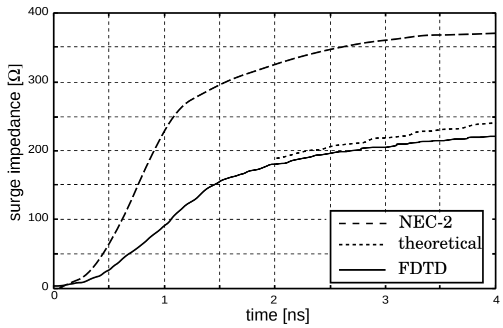

(a) With ground plane.

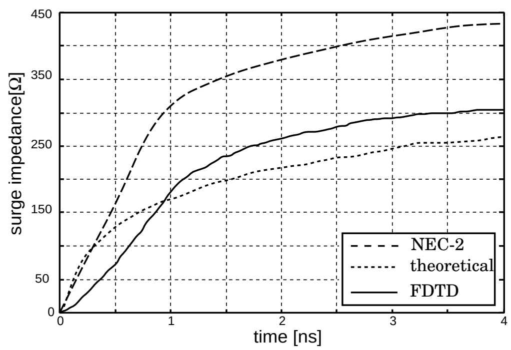

(b) Without ground plane.

Fig. 14. Surge impedance of the single vertical conductor at $0 < t \leq 2h/c$.

$$= 60(\ln(\frac{2\sqrt{2}h}{r_0}) - 1.540). \qquad (21)$$

This formula given by (21) is the same as (20). The waveforms of the surge impedances calculated from the theoretical Equations (19) and (20) with ground and without ground plane respectively, are plotted along with the simulation results by the FDTD method and the MoM in Fig. 14. However, the surge impedance values at $t \approx 2h/c$ are summarized in Table I.

TABLE I
Surge Impedances of the Vertical Conductor at $t \approx 2h/c$

	With ground	Without ground
NEC-2	365	434
Theoretical	232	258
FDTD	214	304

VIII. **CONCLUSIONS**

In this paper, a method of thin wire representation of a vertical conductor system with the effect of ground plane and without ground plane is described. The analysis of surge response has been carried out by the FDTD-based surge simulation code VSTL and MoM-based NEC-2. The accuracy of VSTL has been validated by comparing with NEC-2 results and theoretical values of the vertical conductor surge impedance. The bottom of the analysis space in both cases is considered as a copper plate, although in NEC-2, it was postulated to be on perfectly conducting ground. The analysis results of the surge response with the FDTD method and NEC-2 are found to be quite similar. The computation time absolutely depends on the configuration of the system structures and modeling of the wires.

Acknowledgment: The authors are very much grateful to Dr. T. Noda and S. Yokoyama for their valuable support of utilizing VSTL software for the FDTD calculation and their research contributions.

References

[1] H. W. Dommel, "Digital computer solution of electromagnetic transients in single-and multi-phase networks," *IEEE Trans. Power App. Syst.* , vol. PAS-88, pp. 388–399, Apr.1969.

[2] K. S. Yee, "Numerical solution of initial boundary value problems involving Maxwell's equations in isotropic media," *IEEE Trans. Antennas Propagat.* , vol. AP-14, pp. 302–307, May 1966.

[3] K. S. Kunz and R. J. Luebbers, *The Finite Difference Time Domain Method for Electromagnetics*, Boca Raton, FL: CRC, 1993.

[4] R. F. Harrington, *Field Computation by Moment Methods.* New York: Macmillan, 1968.

[5] G. J. Burke and A. J. Poggio, *Numerical Electromagnetic Code (NEC)– Method of Moments*: Lawrence Livermore Laboratory, 1981.

[6] G. J. Burke and E. K. Miller, "Modeling antennas near to and penetrating a lossy interface," *IEEE Trans. Antennas Propagat.*, vol. AP-32, pp. 1040–1049, Oct. 1984.

[7] T. Noda and S. Yokoyama, "Development of a general surge analysis program based on the FDTD method," *Trans. IEE of Japan* vol. 121-B, no. 5, pp. 625–632, 2001.

[8] H. Takahashi, "A Consideration on the vertical conductor problem," *Proc. of ICEE*, pp. 635–638, 2001.

[9] T. Hara et al., "Transmission tower model for surge analysis," in *Proc. H3 IEE Japan Power and Energy Conf.*, 1991, Paper no. II-270.

[10] M. O. Goni, P. T. Cheng and H. Takahashi, "Theoretical and experimental investigations of the surge response of a vertical conductor," in *Proc. IEEE Power Engineering Soceity Int'n Conf.*, vol. 2, pp. 699–704, 2002.

[11] M. O. Goni, and H. Takahashi, "Theoretical and experimental investigations of the surge response of a vertical conductor," *The ACES Journal*, vol. 18, no. 1 pp. 41–47, Mar. 2003.

[12] K. R. Umashankar et al., "Calculation and experimental validation of induced currents on coupled wires in an arbitrary shaped cavity," *IEEE Trans. Antennas Propagat.*, vol. AP-35, pp. 1248–1248, Nov. 1987.

[13] T. Kashiwa, S. Tanaka, and I. Fukai, "Time domain analysis of Yagi-Uda antennas using the FDTD method," *IEICE Trans. Commun.* vol. J76-BII, pp 872-872, Nov. 1993.

[14] T. Noda and S. Yokoyama, "Thin wire representation in finite difference time domain surge simulation," *IEEE Trans. Power Delivery* vol. 17, no. 3, pp. 840–847, 2002.

[15] Z. P. Liao, H. L. Wong, B.-P. Yang, and Y.-F. Yuan, "A transmitting boundary for transient wave analysis," *Science sinica, Series A,* vol. 27, no. 10 pp. 1063–1063, 1984.

[16] C. A. Jordan, "Lightning computation for transmission line with ground wires," *General Electric Review,* vol. 34, pp. 180–185, 1934.

[17] Y. Baba and M. Ishii, "Numerical electromagnetic field analysis on lightning surge response of tower with shield wire," *IEEE Trans. PWRD,* vol. 15, pp. 1010–1015, no. 3, Jul. 2000.

[18] H. Takahashi, E. Kaneko, K. Yokokura, K. Nojima, T. Shiori, and I. Ohshima, "New Derivation method of the surge impedance on the tower model of a vertical conductor by the electromagnetic field theory (Part 3: Introduction of confined gauge potential and experimental analysis) "(in japanese), *Proc. of IEE of Japan*, vol. 1, pp. 229–234, 1995.

Md. Osman Goni was born in Bangladesh on February, 1971. He received his B.S. degree in electrical and electronic engineering from Bangladesh Institute of Technology, Khulna in 1993. He joined the Institute in 1994. He received M.S. degree from the University of the Ryukyus, Japan in 2001. He is currently a Ph.D. student at the University of the Ryukyus, Japan. His research interests includes electromagnetic theory, the FDTD method, MoM, NEC-2, surge analysis, vertical conductor problems, EMTP etc. He is also a student member of the IEEE, IEE of Japan and AGU.

Eiji Kaneko was born in Japan, on September 16, 1952. He received M.S. degree from Nagoya Univesity in 1977. He joined in Toshiba Corporation in April 1977 and engaged in research and development of vacuum interrupter and discharge. He received D.Eng. degree from Nagoya Univesity in 1989. He is now an associate professor of University of the Ryukyus. He has been engaged in teaching and research on electric power and energy system engineering, electromagnetic energy engineering etc. Dr. Kaneko is a member of IEEE and IEE of Japan.

Hideomi Takahashi was born in Tokyo, Japan, on November 13, 1940. He received B.S. degree from Tokyo Institute of Technology in 1963, and M.S. degree from the University of Tokyo in 1965. He joined in Toshiba Corporation and engaged in the research and development on high voltage engineering, especially vacuum interrupter and ozonizer etc. He received D.Eng. degree from the University of Tokyo in 1986. He is a professor of University of the Ryukyus. He has been engaged in teaching and research on power system engineering. Dr. Takahashi is a senior member of the IEEE and IEE of Japan.